Taylor & Francis
Taylor & Francis Group

Determination of QLNC-3A6 in canine plasma by UHPLC-MS/MS and its application in pharmacokinetic studies

Sumeng Chen[a], Yu Liu[a], Yue Wang[a], Zeyu Wen[a], Jinyan Meng[a], Yuxin Yang[a], Yang Zhang[a], Mei Kong[b], Gang Chen[c] and Xingyuan Cao[a]

[a]Department of Veterinary Pharmacology and Toxicology, College of Veterinary Medicine, China Agricultural University, Beijing, China; [b]Qilu Animal Health Products Co., Ltd., Jinan, Shandong Province, China; [c]School of Food and Health, Beijing Technology and Business University, Beijing, China

ABSTRACT

Multi-targeted tyrosine kinase inhibitor QLNC-3A6 Di-maleate, a structurally novel small molecule compound, has therapeutic efficacy for the treatment of canine cutaneous mast cell tumor (CMCT) caused by mutations in the c-Kit gene. Since pharmacokinetic (PK) information plays an important role in the development and application of new drugs, etc., a rapid, highly sensitive and selective UHPLC-MS/MS analytical method was developed and validated for the first time in this study for the quantitative detection of QLNC-3A6 in canine plasma. 100 μL of plasma was precipitated using 350 μL of acetonitrile, and Chromatographic separation was performed on a Phenomenex Kinetex C18 column (50×2.1 mm, 2.6 μm) at a flow rate of 0.4 mL/min, the mobile phases were set to 0.1% formic acid aqueous solution (A) and 0.1% formic acid acetonitrile (B). The calibration curve linear range was 0.5–100 ng/mL ($R^2 > 0.99$). The intraday and interday precision values (relative standard deviation, RSD) were 2.06–13.57% and 6.90–9.14%. Intraday and interday accuracies were −10.73 to 9.54% and −3.86 to 0.70% respectively. The dilution integrity RSD value and stability RSD value were less than 3.77 and 7.45%, respectively. Subsequently, the pharmacokinetics were investigated in canine after oral administration of QLNC-3A6 Di-maleate tablets at a dose of 3 mg/kg BW using this method. The results showed that QLNC-3A6 showed fast absorption rate, rapid distribution and slow metabolic elimination in canine plasma. The results of the main PK parameters including λz, $T_{1/2\lambda z}$, C_{max}, T_{max} and AUC_{last} were 0.07±0.01/h, 11.00±2.57 h, 50.88±31.94 ng/mL, 9.08±11.57 h and 836.48±230.53 ng h/mL, respectively.

Introduction

In recent years, with the rise in the number of pet canines and the rapid development of animal medical conditions, the lifespan of pet canines has been extended, however, the cancer rate of canines with extended lifespan has also risen (Vascellari et al. 2016). Therefore, drugs for the treatment of canine tumors are urgently needed. Targeted therapy for different subtypes of tumors is the main direction for the future development of antitumor drugs, and targeted therapeutic agents are the main means of personalized treatment (Dobson and Scase 2007). Currently, more and more pharmaceutical companies and research institutes are committed to the research and development of new antitumor targeted therapeutics (Yancey, Merritt, White, et al. 2010) or different formulations (Liu et al. 2024), so as to achieve a more precise and rapid treatment. Meanwhile, the pathogenesis of some tumors is similar in humans and animals (Patruno et al. 2014; Vascellari et al. 2016; Simpson et al. 2017). For example, CMCT, the third most common tumor subtype and the most common malignant skin tumor in canines, accounts for 11% of canine skin cancer cases (de Nardi et al. 2022). Its malignancy rate can be as high as 19–39% (Ma et al. 2021). CMCT is a tumor driven by the cell surface protein tyrosine kinase c-Kit, and CMCT pathogenesis has been associated with mutations in the c-Kit gene (Yancey, Merritt, Lesman, et al. 2010; Bonkobara 2015; Ferguson et al. 2016), which is similar to the mechanism of c-Kit mutations found in human gastrointestinal stromal tumors (GIST) (Patruno et al. 2014). Therefore, the conversion of human drugs to veterinary drugs is now also becoming a new drug research direction.

Qilu Animal Health Products Co., Ltd. has developed a small molecule compound of new structure,

QLNC-3A6 Di-maleate, a small molecule tyrosine kinase inhibitors (TKI) with a mechanism of action similar to that of the marketed drugs including imatinib mesylate (Gleevec, STI571), sunitinib malate (Sutent, SU11248), toceranib phosphate (Palladia, SU11654), and other drugs. The structure of QLNC-3A6 Di-maleate is similar to that drug structure of sunitinib malate, a molecularly modified version of sunitinib malate (Figure 1). However, QLNC-3A6 Di-maleate is a multi-targeted drug, compared with single-targeted drugs, multi-targeted drugs can avoid the disadvantages such as limited efficacy, drug resistance and having potential drug-drug interactions that occur when multiple single-targeted drugs are combined (Raghavendra et al. 2018). And QLNC-3A6 Di-maleate has a favorable safety profile, unlike anticancer drugs with cytotoxic classes (Liu et al. 2024).

The acquisition of PK information occupies an important role in the development and application of new drugs. For QLNC-3A6 analogues several assays are now available. Such methods as LC-MS/MS or UPLC-MS/MS (Tang et al. 2020; Zhang et al. 2022) can be used for the determination of imatinib (Caterino et al. 2013; Xu et al. 2019), sunitinib (AboulMagd and Abdelwahab 2021) and toceranib (TOC) (Yancey, Merritt, Lesman, et al. 2010), among others. At the same time there are now a large number of studies on similar drugs for canine tyrosine kinase-driven different tumours such as insulinomas (Sheppard-Olivares et al. 2022) and pancreatic adenocarcinoma (Musser and Johannes 2021). To the best of our knowledge, there are now studies on pharmacokinetic properties, distribution, metabolism and excretion of the relevant components in CMCT affected dogs administered at a dose of 3.25 mg/kg BW toceranib phosphate (Yancey, Merritt, Lesman, et al. 2010). However, there is no method to detect QLNC-3A6 in canine plasma, so there is an urgent need to develop a rapid and accurate method to detect QLNC-3A6 in canine plasma. The present study aims to explore and establish a sensitive, accurate, and rapid method for the quantification of QLNC-3A6 in canine plasma, and to carry out a complete validation of the method, which was successfully applied to a single oral dose of QLNC-3A6 Di-maleate tablet 3 mg/kg BW after a PK study of QLNC-3A6 in canine plasma. Among them, toceranib phosphate was selected as the internal standard (IS) drug for this study due to its better stability and the fact that CMCT-related studies have been performed (Figure 2).

Materials and methods

Chemicals and reagents

QLNC-3A6 Di-maleate standard (Lot No.25271003GS, purity 99.0%) was supplied by Qilu Animal Health Products Co., Ltd. (China). Toceranib phosphate standard (CAS 874819-74-6, purity 95.07%, internal standard, IS) was purchased from Shandong Link Bio-technology Co., Ltd (China). HPLC grade acetonitrile (ACN) and formic acid (FA) were purchased from Fisher Scientific (USA). Water was purified with Milli-Q water purification system (USA).

Configuration of stock solutions, working solutions, calibration standards and QC samples

Precisely weigh a certain amount of QLNC-3A6 Di-maleate and toceranib phosphate control, respectively, and dissolve them with 50% aqueous acetonitrile to obtain 1.0 mg/mL of stock standard solution (Stock-STD), stock internal standard solution (Stock-IS) and stock control stock solution (Stock-QC), respectively, and store them at −20 °C temperature.

Stock-STD and Stock-QC were diluted with 50% aqueous acetonitrile to obtain QLNC-3A6 series standard sample working solution (W-STD) at concentrations of 5, 20, 50, 100, 200, 500 and 1000 ng/mL, QLNC-3A6 Di-maleate series standard sample working solution (W-STD) at concentrations of 10, 400 and 800 ng/mL, respectively. QLNC-3A6 series quality control sample working solution (W-QC) and internal standard working solution (W-IS) at a concentration of 100 ng/mL.

A precision volume of 90 μL of canine blank plasma was taken, and 10 μL of W-STD and 10 μL of W-QC were added serially to obtain corrected standard samples at concentrations of 0.5, 2, 5, 10, 20, 50, and 100 ng/mL, and quality control samples of LLOQ, LQC, MQC, and HQC at concentrations of 1, 40, and 80 ng/mL, respectively.

UHPLC-MS/MS analysis

An ultra performance liquid chromatography tandem mass spectrometer (UHPLC-MS/MS, Agilent-6470-1260) was used for this analytical method. Chromatographic

QLNC-3A6 Di-maleate a
Chemical Formula: $C_{23}H_{28}FN_5O_2$
Molecular Weight: 657.64

Sunitinib Malate b
Chemical Formula: $C_{26}H_{33}FN_4O_7$
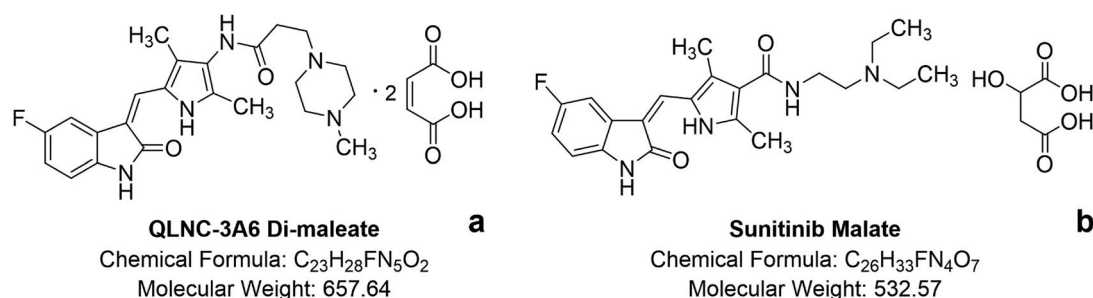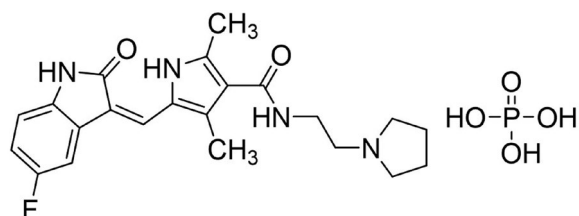Molecular Weight: 532.57

Figure 1. Molecular structural formula of (a) QLNC-3A6 Di-maleate and (b) sunitinib malate.

Toceranib Phosphate
Chemical Formula: $C_{22}H_{28}FN_4O_6P$
Molecular Weight: 494.46

Figure 2. Molecular structural formula of toceranib phosphate.

separation was performed on a Phenomenex Kinetex C18 column (50×2.1 mm, 2.6 μm) at a flow rate of 0.4 mL/min and a temperature of 40 °C. The samples were kept at 8 °C in an autosampler. The mobile phase consisted of 0.1% formic acid aqueous solution (A) and 0.1% formic acid acetonitrile (B). The optimization gradient was as follows: 10% B, 0–0.5 min; 10–50% B, 0.5–3.0 min; 50–90% B, 3.0–3.3 min; 90% B, 3.3–5.0 min; 90–10% B, 5.0–5.3 min; 10% B, 5.3–6.0 min.

Drug quantification was performed by multiple reaction monitoring (MRM) in positive ion electrospray (ESI) mode. The optimized ESI source parameters were as follows: drying gas temperature: 320 °C; sheath gas temperature: 320 °C; nebulizing gas pressure: 45 psi; capillary voltage: 3500 V; and sheath gas flow rate: 11 L/min. The MRM precursor-to-product transitions for QLNC-3A6 and TOC were *m/z* 426.2 > 113.1*, *m/z* 426.2 > 70.2 and *m/z* 397.3 > 283.3*. (*Note*: *is a quantitative ion)

Animals

Six healthy male and female Beagles weighing 8.50–11.50 kg and aged 1.5–2 years were purchased from the Laboratory Animal Center of China Agricultural University. All animals were acclimatized in an environmentally controlled rearing room (temperature 18–25 °C, humidity 30–60%, light and dark cycle every 12 h) for 7 days with free access to food and water. Before the experiment, the canines were fasted for 12 h but had free access to water. Animal experiments were conducted in accordance with the Guidelines for the Breeding and Use of Laboratory Animals and were approved by the Animal Breeding and Use Committee of China Agricultural University (NO.11359-18-E-001) (Beijing, China).

Sample preparation

Frozen plasma samples were thawed at room temperature for about 20 min, vortexed, 100 μL of accurately aspirated plasma samples were transferred to Eppendorf centrifuge tubes, 10 μL of W-IS was added accurately, vortexed, 350 μL of ACN was added to precipitate the proteins, and 250 μL of purified water was added and mixed for 5 min after vortexing, and then centrifuged for 10 min at 4 °C with relative centrifugal force (RCF) 11180 × g, 10,000 rpm. The supernatant

was passed through 0.22 μm organic microporous membrane, vortexed and mixed well, and 3 μL of the supernatant was used for UHPLC-MS/MS analysis.

Method validation

Method validation was performed in accordance with the bioanalytical method validation guidelines of the U.S. Food and Drug Administration (FDA), the European Medicines Agency (EMA 2024), and the Ministry of Agriculture and Rural Affairs of the PRC (EMA 2024; FDA 2024; Veterinary Drug Evaluation Center MoAaRD 2024). At the same time, the International Council for Harmonization of Technical Requirements for Pharmaceuticals for Human Use (ICH) M10 Guideline "Validation of Bioanalytical Methods and Analysis of Research Samples" was used as reference.

Selectivity

To ensure that the established analytical method can be used to differentiate QLNC-3A6 and IS from endogenous components in the matrix or other components in the sample, selectivity should be demonstrated using a suitable blank matrix from at least 6 canines. The response of the interfering component should be less than 20% of the lower limit of quantitation response of the analyte and less than 5% of the internal standard response.

Carry-over

Residues are evaluated by determining the Upper Limit of Quantification (ULOQ) standard sample followed by a double blank (DBK). Residues of QLNC-3A6 should not exceed 20% of the Lower Limit of Quantification (LLOQ) and not exceed 5% of the IS.

Standard curve and LLOQ

After the calibration standard sample was processed, the best-fit curve was generated based on the measured peak area of QLNC-3A6, and linear regression was performed using the least squares method with the weights selected to be $1/x^2$, and at least 6 standard curves were selected for method validation. The calibration standards should be back-calculated to within ±15% of the labeled value, the LLOQ shall be within ±20%, and at least 75% of the calibration standards should contain a minimum of 6 valid concentrations, and the signal-to-noise ratio (S/N) of the LLOQ should be at least 10 times higher than that of the blank sample.

Precision and accuracy

Intra- and inter-batch precision and accuracy were analyzed within one day and on three consecutive days using LLOQ and QC samples (0.5, 1, 40 and

80 ng/mL), respectively. Precision was expressed as the relative standard deviation (RSD) (coefficient of variation, CV) of the measured values and was calculated as the average of standard deviation/average estimated value × 100. Accuracy is expressed in terms of deviation and is calculated as: (measured value/true value) ×100%. For intra-batch precision/accuracy, both require at least 4 concentrations from one analytical batch, with at least 5 samples per concentration; for inter-batch precision/accuracy, both require at least 4 concentrations from 3 analytical batches (at least 2 days), with at least 5 samples per concentration. The CV shall not exceed 15% for QC samples within/between batches and 20% for LLOQ; intra/inter-batch accuracy shall be within ±15% for QC samples and ±20% for LLOQ.

Matrix effect

HQC and LQC matrix effect samples of QLNC-3A6 were prepared using canine blank plasma from 6 batches of different sources. The peak areas of QLNC-3A6 and IS in the matrix were determined after treatment and compared with the corresponding peak areas of pure solution samples without matrix at the corresponding concentrations after treatment. The matrix factors (MF) of QLNC-3A6 and IS were calculated, and then the IS normalized matrix factor (ISnorm-MF) was calculated by dividing the MF of QLNC-3A6 by the MF of IS. The CV of the ISnorm-MF calculated from 6 batches of matrix should not be greater than 15%.

Recovery

Three concentrations of QC samples, LQC (1 ng/mL), MQC (40 ng/mL) and HQC (80 ng/mL), six parallels for each concentration, were processed and injected to determine the peak areas of QLNC-3A6 and IS, and the recoveries were calculated by comparing with the corresponding peak areas of the recovery samples injected for determination of the recoveries of QLNC-3A6 and IS, respectively.

Dilution reliability

Canine plasma samples containing QLNC-3A6 were diluted 2-fold and 10-fold with blank canine plasma, respectively, and analytes need to be above the upper limit of quantification (LOQ) concentration, with a minimum of 5 determinations required for each dilution factor. The accuracy and precision of the dilution shall be within ±15%.

Stability

The stability of QLNC-3A6 was examined with QC samples that had been left at room temperature (25 °C) for 24 h after treatment, QC samples that had been left under an 8 °C injector for 24 h after treatment, QC samples that had been treated with plasma assayed after three times freeze and thaw, QC samples that had been treated and frozen at −80 °C for 30 days after treatment, and QC samples that had been stored at −20 °C in a standard stock solution for 60 days. The stability of the QC samples were examined using a calibration curve that was based on the standard curve. Standard curves were obtained from freshly prepared calibration standards, and the QC samples were analyzed according to the standard curves, comparing the measured concentrations with the labelled concentrations, and the deviation of the mean value of each concentration from the labeled concentration shall be within ±15%.

Application to PK studies

A single oral dose of QLNC-3A6 Di-maleate tablets at a dose of 3 mg/kg BW was administered to canine after an overnight fast. A blood sample of 2 mL was collected in sodium heparin anticoagulant tubes from the brachiocephalic vein of each canine before and 0.5, 1, 2, 4, 6, 8, 12, 24, 36, 48, and 72 h after the administration of QLNC-3A6 Di-maleate tablets. Plasma samples were centrifuged with RCF 1788×g at 4,000 rpm for 10 min and the supernatants were separated immediately and stored at −80 °C until analysis and detection.

Data acquisition and automatic integration were performed using the Aglient MassHunter Workstation Data Acquisition System software configured for the mass spectrometer; the generated data were analyzed and calculated using the non-compartmental model in WinNonlin 6.4 PK software. The main plasma PK parameters included: elimination rate constant (λz), elimination phase half-life ($T_{1/2\lambda z}$), peak concentration (C_{max}), time to peak (T_{max}), area under the drug-time curve from 0 to the last detection time point (AUC_{last}), area under the drug-time curve from 0 to extrapolated infinity ($AUC_{INF\_}obs$), area under the drug-time curve extrapolated as a percentage of the total area under the drug-time curve (AUC_%Extrap_obs), and mean retention time (MRT_{last}).

Results

Method optimization

UHPLC-MS/MS mass spectrometry method optimization

Firstly, MRM was selected as the detection method in this study to minimize the interference of endogenous molecules in biological matrices. (Tang et al. 2022) Secondly, the positive and negative ion detection modes were compared, and it was found that the signal response of the positive ion mode was significantly better than that of the negative ion mode. Subsequently, several columns were evaluated, including BEH-C18 (100×2.1 mm, 1.7 μm), BEH-HILIC (100×2.1 mm, 1.7 μm), HSS-T3 (150×2.1 mm,

1.78 μm), ZORBAX Eclipse Plus C18 (50×2.1 mm, 1.8 μm) and Phenomenex Kinetex C18 (50×2.1 mm, 2.6 μm), the results showed that the Phenomenex Kinetex C18 (50×2.1 mm, 2.6 μm) column had highest response values (Table 1).

Finally, the pH and buffer of the mobile phase system were optimized. Since both drugs involved in this experiment are alkaline, the pH of the configured buffer can be determined directly from the pKa of the analyte, and then the total buffer correction factor can be calculated based on the correction factor of the alkaline analyte when the organic phase is acetonitrile, and different buffer types compatible with LC-MS systems can be selected according to the total correction factor. Among them, 0.1% formic acid produces a mobile phase with a pH of about 2.7, which has become the preferred buffer substance for LC-MS compatibility class under low pH conditions, and higher concentrations of formic acid can improve the response value, but not too high; ammonium acetate produces a mobile phase with a pH of 3.8–5.8; and although aqueous ammonia is a alkaline solution, for reversed-phase liquid chromatographic separations to retain alkaline compounds, a high pH mobile phase is usually selected to enhance reverse retention, but again, high ammonia concentrations should not be chosen because too high concentration of ammonia can inhibit the positive mode response. The results showed that when the mobile phase consisted of 0.1% formic acid aqueous solution (0.1%FA•H$_2$O) (A) and 0.1% formic acid acetonitrile (0.1%FA•ACN) (B), the peak shapes of the substances to be measured were the best and the response was the highest (Table 2).

Table 1. Results of response value of different columns.

	QLNC-3A6 (426.2 > 113.1) (area)	TOC (397.3 > 283.3) (area)
BEH-C18 (100×2.1 mm, 1.7 μm)	8,432	10,542
BEH-HILIC (100×2.1 mm, 1.7 μm)	2,346	7,500
HSS-T3 (150×2.1 mm, 1.78 μm)	5,749	11,356
ZORBAX Eclipse Plus C18 (50×2.1 mm, 1.8 μm)	6,642	10,013
Phenomenex Kinetex C18 (50×2.1 mm, 2.6 μm)	9,912	13,836

Table 2. Results of response value of different mobile phase system pH and buffers.

	QLNC-3A6 (426.2 > 113.1) (area)	TOC (397.3 > 283.3) (area)
A: H$_2$O; B: ACN	7,855	12,157
A: 0.1%FA•H$_2$O; B: 0.1%FA•ACN	10,039	14,739
A: 0.3%FA•H$_2$O; B: 0.3%FA•ACN	8,325	12,279
A: 10 mmol/L Aqueous ammonia H$_2$O; B: 10 mmol/L Aqueous ammonia CAN	7,539	14,641
A: 10 mmol/L Ammonium acetate H$_2$O; B: 10 mmol/L Ammonium acetate ACN	7,953	13,890

Optimization of sample preparation method

For sample preparation, biomarkers in blood are usually at low concentrations and can be masked by high levels of proteins, of which albumin is one of the most prominent, and ACN or MeOH solution (Tomascova et al. 2019) is often utilized to remove albumin from plasma. In this study, different reagents used to precipitate proteins were compared and the results showed that the best results were obtained when 350 μL ACN was used to precipitate 100 μL of plasma with good recoveries (Table 3).

Therefore, 350 μL ACN was used to precipitate 100 μL plasma for sample preparation, and a Phenomenex Kinetex C18 (50×2.1 mm, 2.6 μm) column was selected for the detection, with 0.1%FA•H$_2$O (A) and 0.1%FA•ACN (B) as the mobile phases, and the elution was run for 6 mins at a column temperature of 40 °C according to the optimal gradient. The final chromatogram with good separation and low background noise could be obtained. Figure 3 shows the mass spectra of QLNC-3A6 and TOC from precursor ions to product ions.

Method validation

Selectivity
The results showed that the peak area of the interfering peak at the retention time of QLNC-3A6 in blank plasma was less than 20% of the corresponding peak area of LLOQ, and the peak area of the interfering peak at the retention time of IS was less than 5% of the peak area of the IS of LLOQ, which was in accordance with the regulations, and the details are shown in Figure 4.

Carry-over
After analytical determination, the peak areas of analyte QLNC-3A6 in the DBK samples after ULOQ were all less than 20% of the corresponding peak areas of LLOQ, and the peak areas of IS did not exceed 5% of the corresponding peak areas of LLOQ.

Calibration curves and LLOQ
A calibration standard curve containing at least six points was constructed by plotting the peak area ratio (QLNC-3A6/TOC, Y) versus the nominal

Table 3. Results of response values of plasma proteins precipitated by different reagents.

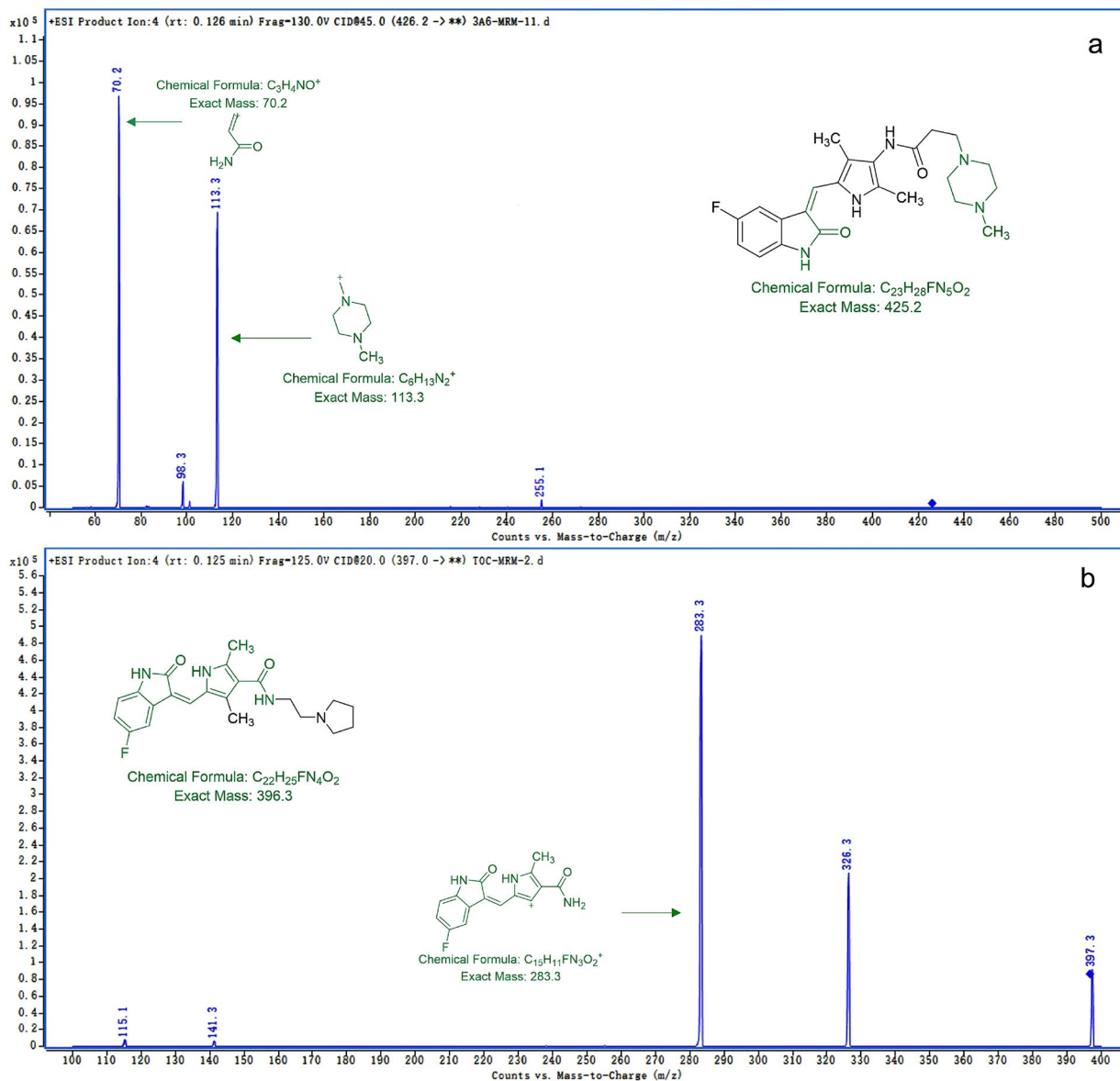|	QLNC-3A6 (426.2 > 113.1) (area)	TOC (397.3 > 283.3) (area)	Recovery (%)
100μL Plasma + 300 μL ACN	5,474	11,729	59.48
100μL Plasma + 350 μL ACN	11,729	15,079	103.27
100μL Plasma + 400 μL ACN	14,751	13,546	133.38
100μL Plasma + 300 μL 0.1%FA•ACN	17,035	15,643	141.02
100μL Plasma + 300 μL MeOH	4,932	9,058	70.64

Figure 3. Mass spectra of (a) QLNC-3A6 and (b) TOC.

concentration of QLNC-3A6 (X) over the range of 0.5–100 ng/mL. The representative regression calibration curve was $y = 0.580138x + 0.013172$ with a weighting factor of $1/x^2$. In each analytical run, good linearity was observed in the regression calibration curve ($R^2 > 0.99$) with %CV < 15. The concentration of LLOQ was 0.5 ng/mL, which showed sufficient precision and accuracy, and the detailed data are shown in Table 4. Meanwhile, the S/N of LLOQ was greater than 10, which met the requirements, and the details are shown in Figure 5.

Precision and accuracy

Table 5 summarizes the intraday and interday precision and accuracy values. It is noteworthy that the intraday and interday %CV were 2.06–13.57% and 6.90–9.14%, respectively. Intraday and interday %DEV were −10.73 to 9.54% and −3.86 to 0.70% respectively. The results indicate that the analytical method is accurate, reproducible and meets the requirements.

Matrix effect

In this experiment, the matrix had a certain inhibition or enhancement effect on the ionization of the analytes, but this effect was not significant ($p > 0.05$), and had little effect on the measurement results. Moreover, the average value of normalized matrix factor of 6 LQC samples of QLNC-3A6 was 95.94%, and the %CV was 4.54%; the average value of normalized matrix factor of 6 HQC samples was 114.81%, and the %CV was 0.85%. The average %CV of the 12 matrix samples at low and high concentrations was 9.78%, which met the relevant requirements. Therefore, the presence of matrix had no effect on the determination of analyte QLNC-3A6.

Recovery

The mean recoveries of analyte QLNC-3A6 in low, medium and high concentration QC samples were 99.72, 102.72 and 102.48%, respectively; and the corresponding mean recoveries of IS were 99.81, 100.89 and 99.71%, respectively. The %CV of analyte and IS
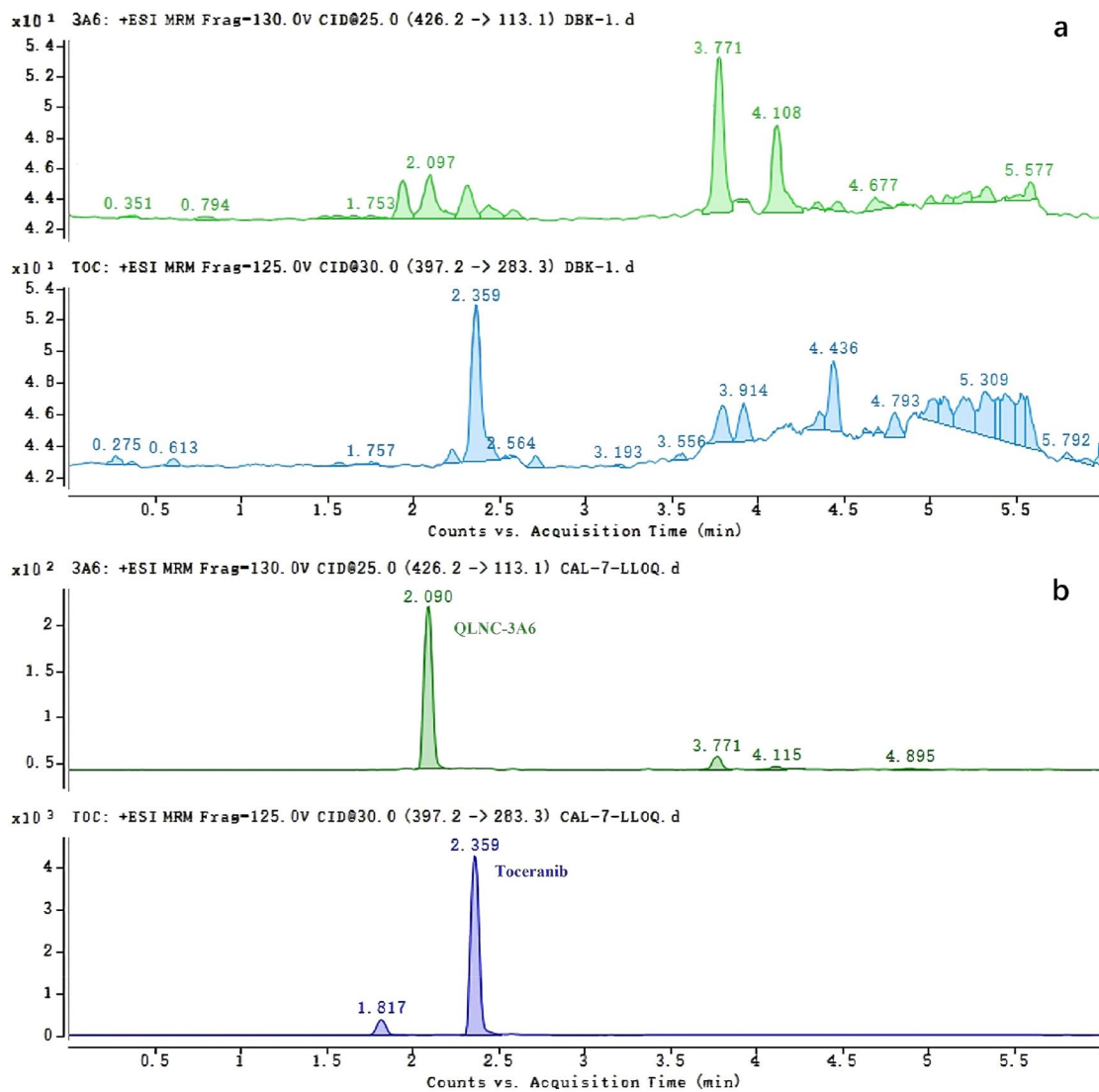
Figure 4. (a) Mass spectra of QLNC-3A6 and TOC in blank canine plasma and (b) plasma spiked to the LLOQ level.

Table 4. Precision and accuracy of the calibration curve back-calculated concentrations and LLOQs ($n=6$).

Concentration(ng/mL)	%DEV	%CV
0.5	0.63	−0.43
2	2.57	0.37
5	3.88	2.34
10	4.59	0.02
20	3.84	2.63
50	2.49	−2.32
100	5.75	−4.51

for 18 QC samples at 3 concentrations ranged from 0.90 to 2.64% and 0.33 to 4.72%, respectively. The recoveries of analytes and IS at low, medium and high concentrations were not much different and basically the same, which satisfied the test requirements.

Dilution integrity
The results of dilution integrity are shown in Table 6. The samples (150 ng/mL) was analyzed with its 2-fold and 10-fold dilutions. The accuracy of analysis of diluted samples was −0.07 to 0.04% with %CV of 3.77 and 2.33%, respectively. The results showed that diluting the plasma samples up to 10-fold did not affect the accurate determination of QLNC-3A6.

Stability
Table 7 lists the stability results for QLNC-3A6 in canine plasma. Stability is defined as the accuracy and precision relative to freshly prepared calibrated plasma samples. It can be seen that the accuracy was −10.92 to 5.05% with %CV < 7.76% under five conditions. The results showed that QLNC-3A6 was stable in the samples that were left at room temperature (about 25 °C) for 24 h after treatment, in the samples that were left under the injector at 8 °C for 24 h after treatment, in the samples that were treated and determined by plasma after three freeze-thawing, and in the samples that were treated by freezing the samples for 30 days at −80 °C. In addition, appropriately diluted standard stock solutions were analyzed, and no significant degradation was observed after 60 days of storage at −20 °C.

PK study
The validated UHPLC-MS/MS analytical method was successfully applied to a preclinical PK study after a single oral dose of QLNC-3A6 Di-maleate tablets in canine at 3 mg/kg BW. Figures 6 and 7 show the
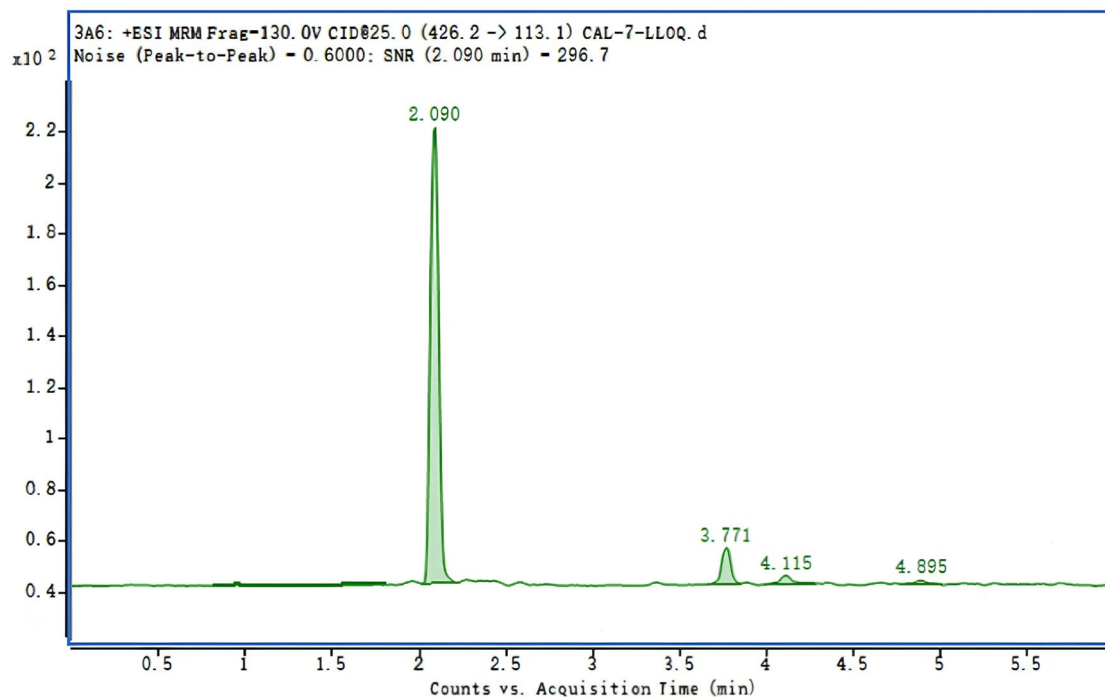
Figure 5. Signal-to-noise chromatogram of LLOQ.

Table 5. Accuracy and precision of QLNC-3A6 determination method in canine plasma.

Concentration (ng/mL)	Intraday ($n=5$ or 6)						Interday ($n=17$ or 18)	
	%DEV	%CV	%DEV	%CV	%DEV	%CV	%DEV	%CV
0.5	−10.73	8.05	−3.75	9.28	1.75	5.90	−3.86	9.14
1	−5.02	9.61	5.75	7.00	1.16	7.85	0.63	8.88
40	−1.74	6.86	−3.26	13.57	0.91	2.83	−1.36	8.46
80	−4.32	2.06	9.54	3.28	−3.13	2.50	0.70	6.90

Note: There were data deviations in the Day1 LLOQ, so the data was eliminated from processing.

Table 6. Dilution integrity of QLNC-3A6 in canine plasma ($n=6$).

Dilution factor	Theoretical concentration (ng/mL)	Measured concentration (ng/mL)	Calculated concentration (ng/mL)	Average concentration (ng/mL)	Accuracy (%DEV)	Precision (%CV)
10X-1	15	14.28955	142.90	144.68	−0.01	2.33
10X-2		14.62599	146.26		0.01	
10X-3		15.06152	150.62		0.04	
10X-4		14.24284	142.43		−0.02	
10X-5		14.44746	144.47		0.00	
10X-6		14.14139	141.41		−0.02	
2X-1	75	69.3356	138.67	148.65	−0.07	3.77
2X-2		75.15666	150.31		0.01	
2X-3		76.21359	152.43		0.03	
2X-4		77.10796	154.22		0.04	
2X-5		73.02266	146.05		−0.02	
2X-6		75.11279	150.23		0.01	

Table 7. Stability of QLNC-3A6 under different storage conditions.

Stability	Concentration(ng/mL)	Mean measured concentration (ng/mL)	Mean accuracy (%DEV)	Precision (%CV)
24h Room temperature (25℃)	1.00	1.00	0.15	6.10
	40	39.74	−0.65	0.18
	80	74.79	−6.52	3.72
24h Injectort (4℃)	1.00	1.00	0.18	7.45
	40	36.11	−9.72	0.71
	80	73.29	−8.39	5.91
Three freeze-thawing (−20℃)	1.00	0.95	−4.57	6.84
	40	40.78	1.96	1.35
	80	75.50	−5.62	3.14
30d Freezing (−80℃)	1.00	0.99	−1.40	5.21
	40	39.57	−1.06	7.76
	80	71.26	−10.92	3.51
60d Stock solution (−20℃)	1.00	1.02	2.31	1.19
	40	82.19	5.05	1.29

mean concentration-time curve and different animals' concentration-time curve of QLNC-3A6 in canine plasma under the Linear Trapezoidal Linear Interpolation (LTLI) calculation. Table 8 lists the main PK parameters calculated using the non-compartmental model. It can be seen from the results that QLNC-3A6 showed fast absorption rate, rapid distribution and slow metabolic elimination in canine plasma. The λz, $T_{1/2\lambda z}$, C_{max}, T_{max} and AUC_{last} were 0.07 ± 0.01/h, 11.00 ± 2.57 h, 50.88 ± 31.94 ng/mL, 9.08 ± 11.57 h and 836.48 ± 230.53 ng h/mL, respectively.

Discussion

From the concentration-time curves of QLNC-3A6 in different canine, it can be found that the curves in multiple animals showed the phenomenon of irregular double or multiple peaks.

According to the relevant literature, oral drugs are susceptible to bimodal absorption phenomenon during gastric emptying to small intestinal absorption process (Mirfazaelian and Mahmoudian 2006) such as ranitidine (Yin et al. 2003), phenazopyridine (Shang et al. 2005), talinolol, paracetamol (Weitschies et al. 2005), and toceranib (Yancey, Merritt, White, et al. 2010). There are many reasons for the bimodal or multimodal phenomenon for such drugs, such as delayed gastric emptying (Weitschies et al. 2005; Metsugi et al. 2008; Ogungbenro et al. 2015), enterohepatic recirculation (EHC) (Marier et al. 2002; Soulele and Karalis 2019), and uneven distribution of the drug efflux transporter protein, P-gp, in the small intestinal (Godfrey et al. 2011; Wada et al. 2013).

For the phenomenon of sub-peak, non-linear PK or slow drug metabolism after the absorption time in the small intestine, it may be due to the individual liver metabolizing the drug to reach the saturation of the flip-flop phenomenon. In turn, the occurrence of flip-flop kinetics phenomenon is related to many factors such as the weak acid ionization equilibrium constant K_a of the drug, elimination rate constant K_{el} (Yáñez et al. 2011) and intestinal transporter substrate (Garrison et al. 2015). According to the literature, the presence of flip-flop
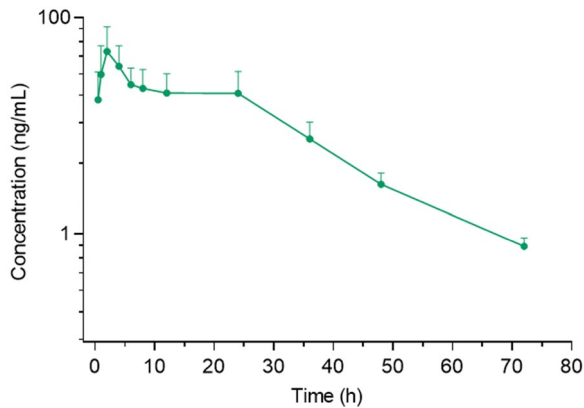

Figure 6. Plasma mean concentration-time curve of QLNC-3A6 di-maleate tablets after a single oral dose of 3 mg/kg BW in canine ($n = 6$).

Table 8. PK parameters of QLNC-3A6 di-maleate tablets after a single oral dose of 3 mg/kg BW in canine ($n = 6$).

Parameters	Unit	Mean ± SD
λz	h^{-1}	0.07 ± 0.01
$T_{1/2\lambda z}$	h	11.00 ± 2.57
C_{max}	ng mL^{-1}	50.88 ± 31.94
T_{max}	h	9.08 ± 11.57
AUC_{last}	ng h mL^{-1}	836.48 ± 230.53
AUC_{INF_obs}	ng h mL^{-1}	851.74 ± 230.17
$AUC\_\%Extrap\_obs$	%	1.96 ± 1.20
MRT_{last}	h	18.63 ± 4.47

λ_z: elimination rate constant; $T_{1/2\lambda z}$: elimination phase half-life; C_{max}: peak concentration; T_{max}: peak time; AUC_{last}: area under the drug-time curve from 0 to the last detected time point; AUC_{INF}_obs, area under the drug-time curve from 0 to extrapolation to infinity; $AUC_{\%Extrap\_obs}$, extrapolated drug-time curve area under the drug-time curve as a percentage of the total area under the drug-time curve percent; MRT_{last}, mean retention time.
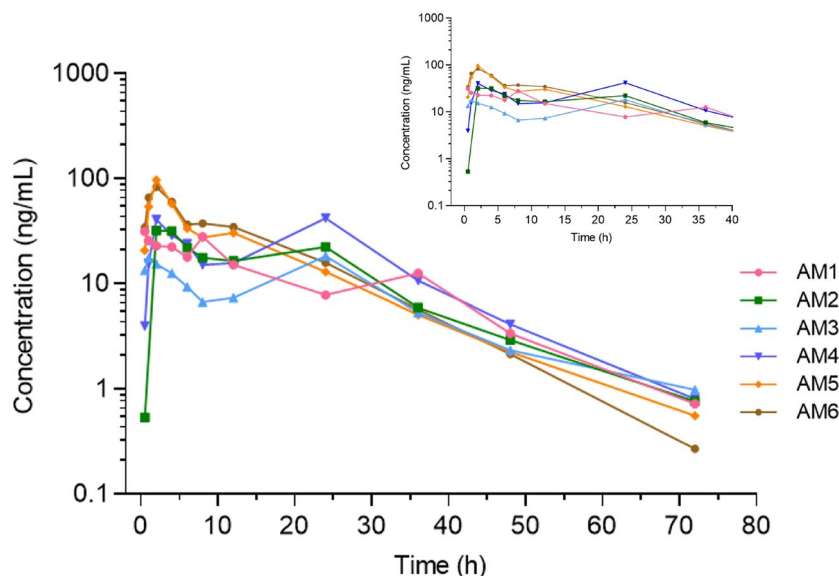

Figure 7. Plasma concentration-time curves in different animals following a single oral dose of QLNC-3A6 Di-maleate tablets at 3 mg/kg BW in canine. A close-up view is shown for the first 36 h post drug administration.

phenomenon may also be accompanied by EHC (Gupta and Gupta 2016).

Based on the current data, it is initially hypothesized that QLNC-3A6 is more variable in canine plasma, and that the double or multiple peaks phenomenon in the drug-time graphs is most likely a result of the EHC, the gastrointestinal tract having multiple absorption points, and the flip-flop. There is also the phenomenon that the generated curve masks more peaks due to the lack of sampling time points.

Therefore, the sampling time points should be rationally adjusted in the following in-depth study of QLNC-3A6 in canine, and related studies such as drug excretion should be carried out.

Conclusion

In this study, a rapid, highly sensitive and selective UHPLC-MS/MS analytical method was developed for the first time for the quantitative detection of QLNC-3A6 in canine plasma. The specificity and sensitivity, linearity and calibration curve, precision and accuracy, dilution integrity and stability of the method meet the requirements of the guidelines of the FDA, EMA and Ministry of Agriculture and Rural Affairs of the PRC. The developed method has significant advantages in terms of simple sample preparation, rapid chromatographic separation and high throughput efficiency. This new approach was also utilized in the present study to investigate the PK of QLNC-3A6 Di-maleate tablets after a single oral dose of 3 mg/kg BW in canine. The results indicated that QLNC-3A6 showed fast absorption rate, rapid distribution and slow metabolic elimination in canine plasma, which is valuable for future exploration of the clinical PK of QLNC-3A6.

Ethical approval

Animal experiments were conducted in accordance with the Guidelines for the Breeding and Use of Laboratory Animals and were approved by the Animal Breeding and Use Committee of China Agricultural University (NO.13303-24-E-001) (Beijing, China).

Author contributions

Corresponding author S.C., Y.L., and Y.W. participated in study design, conceptualization and project management. Qilu Animal Health Products Co., Ltd. provided the QLNC-3A6 Di-maleate. S.C., Z.W. and J.M. assisted in sample collection and clinical observation. M.J., Y.Y., Y.Z. participated in data collection and organization. S.C., Y.L., M.J.,and X.C. responsible for outcome monitoring and evaluation. S.C., M.K., G.C. and X.C. involved in writing the original manuscript, surveys and study execution. All authors have read and agreed to the published version of the manuscript.

Disclosure statement

No potential conflict of interest was reported by the author(s).

Funding

Data availability statement

The data supporting the findings of this study are available from Dr. Sumeng Chen (2676938520@qq.com) upon request.

References

AboulMagd AM, Abdelwahab NS. 2021. Analysis of sunitinib malate, a multi-targeted tyrosine kinase inhibitor: a critical review. Microchemical J. 163:105926. doi: 10.1016/j.microc.2021.105926.

Bonkobara M. 2015. Dysregulation of tyrosine kinases and use of imatinib in small animal practice. Vet J. 205(2):180–188. doi: 10.1016/j.tvjl.2014.12.015.

Caterino M, Casadei GM, Arvonio R, De Francia S, Pirro E, Piccione FM, Pane F, Ruoppolo M. 2013. Quantification of imatinib plasma levels in patients with chronic myeloid leukemia: comparison between HPLC-UV and LC-MS/MS. Int J Pept Res Ther. 19(2):109–116. doi: 10.1007/s10989-012-9321-0.

de Nardi AB, Horta RD, Fonseca-Alves CE, de Paiva FN, Linhares LCM, Firmo BF, Sueiro FAR, de Oliveira KD, Lourenco SV, Strefezzi RD, et al. 2022. Diagnosis, prognosis and treatment of canine cutaneous and subcutaneous mast cell tumors. Cells. 11(4):618–628. doi: 10.3390/cells11040618.

Dobson JM, Scase TJ. 2007. Advances in the diagnosis and management of cutaneous mast cell tumours in dogs. J Small Anim Pract. 48(8):424–431. doi: 10.1111/j.1748-5827.2007.00366.x.

EMA. 2024. Guideline on bioanalytical method validation. E.M. Agency. [accessed 2024 May 9]. https://www.ema.europa.eu/documents/scientific-guideline/guideline-bioanalytical-method-validation_en.pdf.

FDA. 2024. Guidance for industry on bioanalytical method validation. C.f.D.E.a.R. Food and Drug Administration. [accessed 2024 May 9]. https://www.fda.gov/files/drugs/published/Bioanalytical-MethodValidation-Guidance-for-Industry.pdf.

Ferguson MJ, Rhodes SD, Jiang L, Li XH, Yuan J, Yang XL, Zhang SB, Vakili ST, Territo P, Hutchins G, et al. 2016. Preclinical evidence for the use of sunitinib malate in the treatment of plexiform neurofibromas. Pediatr Blood Cancer. 63(2):206–213. doi: 10.1002/pbc.25763.

Garrison KL, Sahin S, Benet LZ. 2015. Few drugs display flip-flop pharmacokinetics and these are primarily associated with classes 3 and 4 of the BDDCS. J Pharm Sci. 104(9):3229–3235. doi: 10.1002/jps.24505.

Godfrey KR, Arundel PA, Dong ZM, Bryant R. 2011. Modelling the double peak phenomenon in pharmacokinetics. Comput Methods Programs Biomed. 104(2):62–69. doi: 10.1016/j.cmpb.2010.03.007.

Gupta PK, Gupta PK. 2016. Principles and basic concepts of toxicokinetics. Fund Toxicol Essen Concepts Appl. 87–107. doi: 10.1016/b978-0-12-805426-0.00009-3.

Liu Y, Chen S, Wen Z, Meng J, Yang Y, Zhang Y, Wang J, Cao X. 2024. Comparative pharmacokinetics of free doxorubicin and a liposomal formulation in cats following intravenous administration. Front Vet Sci. 11:1353775. doi: 10.3389/fvets.2024.1353775.

Ma Y, Xie T, Zhang J, Shi J, Gao R, Xu R, He W, Gao F, Lu H. 2021. Pathological diagnosis and c-kit immunohisto-chemical analysis of three cases of canine cutaneous mast cell tumor. Chinese J Vet Sci. 41:2015–2020.

Marier JF, Vachon P, Gritsas A, Zhang J, Moreau JP, Ducharme MP. 2002. Metabolism and disposition of resveratrol in rats: extent of absorption, glucuronidation, and enterohepatic recirculation evidenced by a linked-rat model. J Pharmacol Exp Ther. 302(1):369–373. doi: 10.1124/jpet.102.033340.

Metsugi Y, Miyaji Y, Ogawara K-i, Higaki K, Kimura T. 2008. Appearance of double peaks in plasma concentration-time profile after oral administration depends on gastric emptying profile and weight function. Pharm Res. 25(4):886–895. doi: 10.1007/s11095-007-9469-z.

Mirfazaelian A, Mahmoudian M. 2006. A simple pharmacokinetics subroutine for modeling double peak phenomenon. Biopharm Drug Dispos. 27(3):119–124. doi: 10.1002/bdd.492.

Musser ML, Johannes CM. 2021. Toceranib phosphate (Palladia) for the treatment of canine exocrine pancreatic adenocarcinoma. BMC Vet Res. 17(1):269. doi: 10.1186/s12917-021-02978-8.

Ogungbenro K, Pertinez H, Aarons L. 2015. Empirical and semi-mechanistic modelling of double-peaked pharmacokinetic profile phenomenon due to gastric emptying. Aaps J. 17(1):227–236. doi: 10.1208/s12248-014-9693-5.

Patruno R, Marech I, Zizzo N, Ammendola M, Nardulli P, Gadaleta C, Introna M, Capriuolo G, Rubini RA, Ribatti D, et al. 2014. C-kit expression, angiogenesis, and grading in canine mast cell tumour: a unique model to study C-kit driven human malignancies. Biomed Res Int. 2014:730246–730248. doi: 10.1155/2014/730246.

Raghavendra NM, Pingili D, Kadasi S, Mettu A, Prasad S. 2018. Dual or multi-targeting inhibitors: the next generation anticancer agents. Eur J Med Chem. 143:1277–1300. doi: 10.1016/j.ejmech.2017.10.021.

Sheppard-Olivares S, Bello NM, Johannes CM, Hocker SE, Biller B, Husbands B, Snyder E, McMillan M, McKee T, Wouda RM. 2022. Toceranib phosphate in the management of canine insulinoma: a retrospective multicentre study of 30 cases (2009–2019). Vet Rec Open. 9(1):e27. doi: 10.1002/vro2.27.

Shang EX, Xiang BR, Liu GY, Xie SF, Wei WY, Lu J. 2005. Determination of phenazopyridine in human plasma via LC-MS and subsequent development of a pharmacokinetic model. Anal Bioanal Chem. 382(1):216–222. doi: 10.1007/s00216-005-3197-1.

Simpson S, Dunning MD, de Brot S, Grau-Roma L, Mongan NP, Rutland CS. 2017. Comparative review of human and canine osteosarcoma: morphology, epidemiology, prognosis, treatment and genetics. Acta Vet Scand. 59(1):71. doi: 10.1186/s13028-017-0341-9.

Soulele K, Karalis V. 2019. On the population pharmacokinetics and the enterohepatic recirculation of total ezetimibe. Xenobiotica. 49(4):446–456. doi: 10.1080/00498254.2018.1463117.

Tang C, Niu X, Shi L, Zhu H, Lin G, Xu RA. 2020. *In vivo* pharmacokinetic drug-drug interaction studies between fedratinib and antifungal agents based on a newly developed and validated UPLC/MS-MS method. Front Pharmacol. 11:626897. doi: 10.3389/fphar.2020.626897.

Tang L, Swezey RR, Green CE, Mirsalis JC. 2022. Enhancement of sensitivity and quantification quality in the LC-MS/MS measurement of large biomolecules with sum of MRM (SMRM). Anal Bioanal Chem. 414(5):1933–1947. doi: 10.1007/s00216-021-03829-z.

Tomascova A, Lehotsky J, Kalenska D, Baranovicova E, Kaplan P, Tatarkova Z. 2019. A comparison of albumin removal procedures for proteomic analysis of blood plasma. Gen Physiol Biophys. 38(4):305–314. doi: 10.4149/gpb_2019009.

Vascellari M, Capello K, Carminato A, Zanardello C, Baioni E, Mutinelli F. 2016. Incidence of mammary tumors in the canine population living in the Veneto region (Northeastern Italy): risk factors and similarities to human breast cancer. Prev Vet Med. 126:183–189. doi: 10.1016/j.prevetmed.2016.02.008.

Veterinary Drug Evaluation Center, M.o.A.a.R.D. 2024. China technical guidelines for the validation of quantitative analytical methods for biological samples. [accessed 2024 May 9]. http://www.ivdc.org.cn/pszx/ywgz/zdyz/sjk/hxy/index_4.htm.

Wada S, Kano T, Mita S, Idota Y, Morimoto K, Yamashita F, Ogihara T. 2013. The role of inter-segmental differences in P-glycoprotein expression and activity along the rat small intestine in causing the double-peak phenomenon of substrate plasma concentration. Drug Metab Pharmacokinet. 28(2):98–103. doi: 10.2133/dmpk.DMPK-12-RG-005.

Weitschies W, Bernsdorf A, Giessmann T, Zschiesche M, Modess C, Hartmann V, Mrazek C, Wegner D, Nagel S, Siegmund W. 2005. The talinolol double-peak phenomenon is likely caused by presystemic processing after uptake from gut lumen. Pharm Res. 22(5):728–735. doi: 10.1007/s11095-005-2588-5.

Xu RA, Lin Q, Qiu X, Chen J, Shao Y, Hu G, Lin G. 2019. UPLC-MS/MS method for the simultaneous determination of imatinib, voriconazole and their metabolites concentrations in rat plasma. J Pharm Biomed Anal. 166:6–12. doi: 10.1016/j.jpba.2018.12.036.

Yancey MF, Merritt DA, Lesman SP, Boucher JF, Michels GM. 2010. Pharmacokinetic properties of toceranib phosphate (Palladia™, SU11654), a novel tyrosine kinase inhibitor, in laboratory dogs and dogs with mast cell tumors. J Vet Pharmacol Ther. 33(2):162–171. doi: 10.1111/j.1365-2885.2009.01133.x.

Yancey MF, Merritt DA, White JA, Marsh SA, Locuson CW. 2010. Distribution, metabolism, and excretion of toceranib phosphate (Palladia (TM), SU11654), a novel tyrosine kinase inhibitor, in dogs. J Vet Pharmacol Ther. 33(2):154–161. doi: 10.1111/j.1365-2885.2009.01120.x.

Yáñez JA, Remsberg CM, Sayre CL, Forrest ML, Davies NM. 2011. Flip-flop pharmacokinetics-delivering a reversal of disposition: challenges and opportunities during drug development. Ther Deliv. 2(5):643–672. doi: 10.4155/tde.11.19.

Yin OQP, Tomlinson B, Chow AHL, Chow MSS. 2003. A modified two-portion absorption model to describe double-peak absorption profiles of ranitidine. Clin Pharmacokinet. 42(2):179–192. doi: 10.2165/00003088-200342020-00005.

Zhang Y, Liu YN, Xie S, Xu X, Xu RA. 2022. Evaluation of the inhibitory effect of quercetin on the pharmacokinetics of tucatinib in rats by a novel UPLC-MS/MS assay. Pharm Biol. 60(1):621–626. doi: 10.1080/13880209.2022.2048862.